Biochemistry and Biophysics Reports 24 (2020) 100842

Contents lists available at ScienceDirect

Biochemistry and Biophysics Reports

journal homepage: www.elsevier.com/locate/bbrep

# Biocompatibility analysis of high molecular weight chitosan obtained from *Pleoticus muelleri* shrimps. Evaluation in prokaryotic and eukaryotic cells

Mariana Carolina Di Santo [a,b,1], Agustina Alaimo [a,b,1], Ana Paula Domínguez Rubio [a,b], Regina De Matteo [a,b], Oscar Edgardo Pérez [a,b,*]

[a] Departamento de Química Biológica, Facultad de Ciencias Exactas y Naturales, Universidad de Buenos Aires, Buenos Aires, Argentina
[b] Instituto de Química Biológica de La Facultad de Ciencias Exactas y Naturales, Universidad de Buenos Aires, Consejo Nacional de Investigaciones Científicas y Técnicas, Buenos Aires, Argentina

ARTICLE INFO

*Keywords:*
Chitosan
Biocompatibility
*Lactobacillus casei*
3T3-L1
Caco-2
ARPE-19
EA.hy926

ABSTRACT

The search for the exploitation and recycling of biomaterials is increasing for reducing the use of non-renewable resources and minimizing environmental pollution caused by synthetic materials. In this context, Chitosan (CS) being a naturally occurring biopolymer becomes relevant. The aim of the present work was to explore the effects of High Molecular Weight CS (H-CS) from Argentinean shrimp's wastes in prokaryotic and eukaryotic *in vitro* cell cultures. Ultrastructure of H-CS was analysed by SEM and TEM. *In vitro* studies were performed in prokaryotic *(Lactobacillus casei* BL23*)* and eukaryotic (Caco-2, ARPE-19, EA.hy926 and 3T3-L1) culture cells. High performance microscopic techniques were applied to examine culture cells. No changes in morphology were found in any of the cell types. In addition, fluorescent-dyed H-CS revealed that eukaryotic cells could internalize it optimally. Viability was maintained and proliferation rate even increased for Caco-2, ARPE-19 and 3T3-L1 cells under H-CS treatment. Besides, viability was neither altered in *L. casei* nor in EA.hy926 cells after H-CS exposure. In conclusion, H-CS could be a suitable biopolymer to be exploited for biomedical or food industry applications.

## 1. Introduction

A biomaterial is regarded to any natural or synthetic substance in origin, able to treat, improve or supplant tissue, organ, or functions in biological systems [1,2]. Biomaterials also refer to biologically derived raw materials applied primarily for their structural rather than biological properties. Also, biomaterials play an increasing role in modern health care systems [3].

Biological evaluation of biomaterials is central to the International Standard (ISO 10993–5), which does not specify a single test, but rather attempts to present guidelines for the choice of suitable assessments such as: cell damage by morphological means, measurements of cell growth and/or specific aspects of cellular metabolism. All these techniques correspond to a classical approach, although they are internationally accepted [4].

Carbohydrates are versatile biomaterials because of their interactions with other biomolecules [1,5]. In this sense, polysaccharides are complex carbohydrates which are considered optimal biomaterials [6,7]. Particularly, marine-derived polysaccharide have attracted attention for their wide usefulness in the biotechnological field [8]. Oceans contain several marine organisms, including algae, animals and plants, from which diverse polysaccharides with useful properties can be obtained [9,10]. Ever since ancient time, there are several attempts to reduce the volume of marine waste material with the aim to turn it into useful products [11]. That is the case for the obtaining and recycling of chitin, the second most abundant polysaccharides on Earth after cellulose [10,12].

Chitin is an organic polymer whose main natural sources are crustaceans (e.g. crabs, shrimps and lobsters), insects, molluscs, and the cell walls of certain fungi [11]. Despite the reduced applications of chitin, there is an expanding interest from the pharmaceutical and biomedical areas, food industry as well as materials science, among others, since it can be converted into chitosan (CS) through a deacetylation process [13,14].

CS is a linear polysaccharide whose structure is comprised of β-1,4-linked 2-amino-2-deoxy-β-D-glucose (deacetylated D-glucosamine) and

* Corresponding author. Departamento de Química Biológica, Facultad de Ciencias Exactas y Naturales, Universidad de Buenos Aires, Buenos Aires, Argentina.
*E-mail addresses:* cdisanto@qb.fcen.uba.ar (M.C. Di Santo), aalaimo@qb.fcen.uba.ar (A. Alaimo), apaudr@qb.fcen.uba.ar (A.P. Domínguez Rubio), rdematteo@qb.fcen.uba.ar (R. De Matteo), oscarperez@qb.fcen.uba.ar, oscarperez@gmail.com (O.E. Pérez).
[1] These authors contributed equally to this work.

https://doi.org/10.1016/j.bbrep.2020.100842
Received 17 August 2020; Received in revised form 19 October 2020; Accepted 27 October 2020

*N*-acetyl-D-glucosamine units [15,16]. The presence of $–NH_2$ and –OH groups in the CS structure gives it interesting chemical and biological properties. Biodegradable, biocompatible, and antimicrobial properties were described for CS [14,17]. In particular, biocompatibility or absent of cytotoxicity is one of the main prerequisites for biomaterials whose destination will be the application in biological systems, e.g. human body [18]. By definition, biocompatibility involves the exclusion of toxic or harmful effects of the biomaterial on the biological systems [4,19]. Central to the biocompatibility analysis is the cytotoxicity, which can be tested *in vitro* by employing an array of various target primary cells or cell lines. The possible effect of toxic agents on cellular functions and cell viability could be branded by changes in the type-specific cellular morphology, loss of cell adhesion, reduced cellular proliferation and cell death [18].

Although CS exhibited more than a few advantages over other synthetic biomaterials for its easy manipulation and low cost of obtaining and production, most of scientific reports refer almost only to commercial low molecular weight (MW) CS, i.e. analytical grade. That is to say, outside of those, another type of CS was poorly studied.

The aim of the present work was to explore the effects of a novel High MW CS (H-CS) in prokaryotic and eukaryotic cell models. Particularly, the biocompatibility of H-CS was analysed here. This polysaccharide was obtained from chitin of *Pleoticus muelleri* shrimp wastes, the main crustacean exploited in Mar del Plata, Argentine maritime platform of the Atlantic Ocean [16,20,21]. Those marine exoskeleton wastes are environmental pollutant, but these raw materials could be useful for obtaining of beneficial products for health. In the present study, the hypothesis raised implies that H-CS would not exert cytotoxicity in the tested cell cultures.

## 2. Materials and methods

### 2.1. Reagents

H-CS (300 kDa) was provided by the Microbiology Laboratory of National Institute of Industrial Technology (INTI) (Mar del Plata, Buenos Aires, Argentina), in the frame of a joint project with our laboratory. Fetal Bovine Serum (FBS), 3-(4,5-dimethyl-thiazol-2-yl)-2,5-diphenyl-tetrazolium bromide (MTT) was from Sigma-Aldrich Co. (St. Louis, USA). Crystal violet was from Merck Millipore Corp. (Darmstadt, Germany). Trypan Blue powder (CAS 72-57-1) (sc-216028) was purchased from Santa Cruz Biotechnology Inc. (Santa Cruz, USA). MRS was from Biokar Diagnostics (Beauvais, France) and 5 (6)-carboxyfluorescein diacetate *N*-succinimidyl ester (CFSE) from Invitrogen (Thermo Fisher Scientific Inc., USA). Dulbecco's Modified Eagle's Medium (DMEM), Trypsin-EDTA 0.5%, Antibiotic-Antimycotic (penicillin, streptomycin, and Amphotericin B) and GlutaMAX™-l (L-alanine-L-glutamine) were from Gibco (Thermo Fisher Scientific, Inc., MA, USA). Other chemicals used were of analytical grade. Ultrapure quality water was used.

### 2.2. H-CS solutions

H-CS was purified before its use according to the protocol previously described [16,20]. In a preceding study of our group, the viscosity-average MW of chitosan was determined (300 KDa). Deacetylation degree of CS was determined by elemental analysis [20,22]. After H-CS washing, 0.1 g of powder was dissolved in 10 mL of $CH_3COOH$ solution 1% (v/v) or HCl 0.1 M solution in ultra-pure water under continuous stirring for 24 h. The solution was centrifuged (1000 RPM, 15 min) and the supernatant collected for further studies.

### 2.3. Ultrastructure analysis

#### 2.3.1. Scanning electron microscopy (SEM)

Samples were frozen for 24 h at −20 °C in glass vials. Then, samples were freeze-dryed for 48 h on an Alpha 1–4 LD/2–4 LD-2 lyophilizer (Martin Christ Gefriertrocknungsaniagen GmbH, Germany) operated at a pressure of 4 Pa and a temperature of −54 °C. SEM images were obtained using a Carl Zeiss NTS - SUPRA 40 (Zeiss, Germany) with an accelerated voltage of 3 kV. Powdered samples were sprinkled onto a two-sided adhesive tape and then coated with a thin layer of gold.

#### 2.3.2. Transmission electron microscopy (TEM)

Analysis was carried out according to Ref. [23]. Samples (10 μl) were diluted in ultra-pure water (1:100 v/v). Then, 10 μL of the diluted sample was mixed 1:1 with 1% (w/v) uranyl acetate. An aliquot was placed onto a copper grid covered with a Formvar® film (200 mesh). Liquid excess was eliminated using a filter paper and the grids were dried in a desiccator. Imaging was performed using MET Zeiss 109 with a Gatan W10000 camera (Carl Zeiss NTS GmbH, Germany). Representative SEM and TEM images were analysed using 3D Surface Plot (Fiji software, NIH) [24].

### 2.4. Cell cultures and treatments

#### 2.4.1. Prokaryotic cells

The probiotic strain *Lactobacillus casei* BL23 was grown in MRS broth medium at 37 °C (100 mL of fresh medium were inoculated with an aliquot of the preculture to obtain a $DO_{600nm} = 0.15$). When the culture reached a $DO_{600nm} = 0.5$ (log phase of growth), aliquots of 100 μL of culture were incubated with 10 μL of H-CS solutions at 37 °C for 1 h [25]. For that purpose, H-CS 1% (w/v) was previously diluted with PBS or $CH_3COOH$ solution 1% (v/v) to obtain the final concentrations (0.5, 50 and 500 μg/mL). The Colony Forming Units per milliliter (CFU/ml) were determined by plating on MRS agar plates and incubation for 48 h at 37 °C.

Living bacteria were stained with CFSE at 10 mM final concentration in PBS for 30 min at 37 °C. After washing three times in PBS, by centrifuging at 4 °C and 4000 g for 5 min each time, the samples were visualized by Confocal Laser Scanning Microscopy (CLSM) using an Olympus FV1000 module (Olympus, Japan) [25].

#### 2.4.2. Eukaryotic cells

Mouse fibroblast 3T3-L1 (ATCC®CL-173™), human intestinal epithelial Caco-2 (ATCC®HTB-37™), human retinal pigment epithelial ARPE-19 (ATCC®CRL-2302™) and human endothelial EA.hy926 (ATCC®CRL-2922™) cell lines were grown in DMEM supplemented with 10% heat-inactivated FBS, 2.0 mM glutamine, 100 units/mL penicillin, 100 μg/mL streptomycin and 0.25 μg/mL amphotericin. Cells were maintained at 37 °C in a humidified atmosphere of 5% $CO_2$. Medium was renewed three times per week. Cells were detached with 0.05% Trypsin-EDTA in PBS, diluted with DMEM 10% FBS and re-plated into multi-well plates to yield 70–80% confluent cultures.

For MTT and Crystal violet assays, 3T3-L1, Caco-2, EA.hy926 and ARPE-19 cells were seeded at $2 \times 10^4$ cells/well in 96-well culture plates. After 24 h, culture media was discarded and cells were incubated for 48 h with 50 μg/mL of H-CS in 10% FBS fresh culture media at 37 °C, 5% $CO_2$.

For Trypan Blue assay, cells were seeded at a density of $5 \times 10^4$ cells/well in 48-well culture plates. After 24 h, cells were treated with H-CS and the number of initial live cells were counted and registered by TB method (0 h). Subsequently, live cells were counted after 24 and 48 h of H-CS treatment application.

### 2.5. Cell proliferation and viability assays

#### 2.5.1. MTT assay

The MTT assay is a colorimetric assay for assessing cell metabolic activity. The conversion of MTT to formazan by mitochondrial dehydrogenases was utilized as an index of cell viability. MTT assay was measured as described before [26,27]. Formazan absorbance was measured at 570 nm with background subtraction at 690 nm on a

POLARstar Omega microtiter plate reader (BMG LABTECH, Germany). Controls were considered 100%.

### 2.5.2. Crystal violet assay

Crystal violet assay (CV) is one of the common methods used to detect cell viability or drug cytotoxicity. CV is a triarylmethane dye that binds to DNA and proteins. Usually, under injury, dead adherent cells will detach from cell culture plates and will be eliminated from viable cell population through washing steps. Consequently, CV staining is directly proportional to the cellular biomass. This assay was carried out according to the protocol previously described [18,19]. The CV absorbance was measured at 570 nm with background subtraction at 690 nm on a POLARstar Omega microplate reader (BMG LABTECH, Germany). Controls were considered 100%.

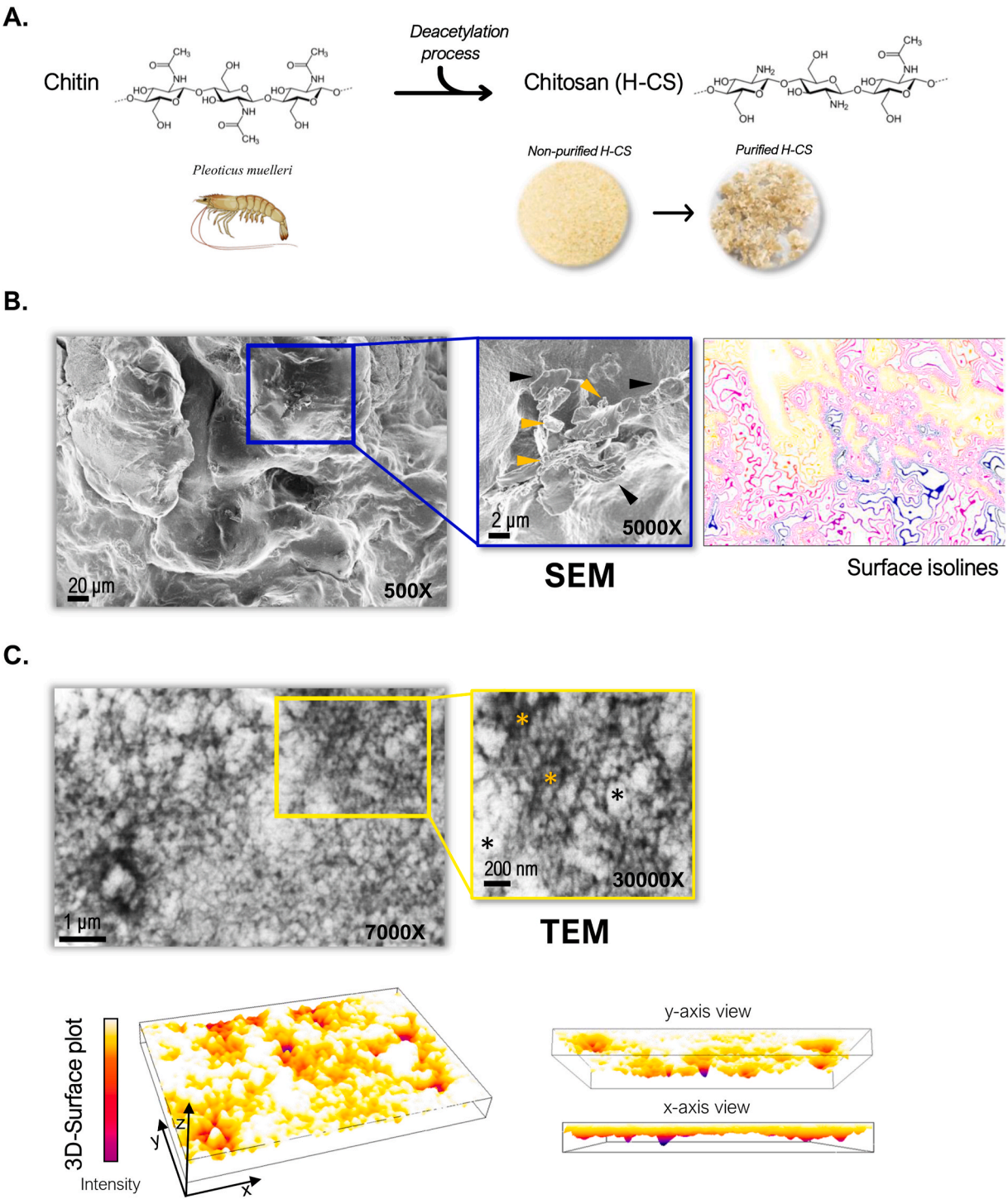


**Fig. 1. A.** H-CS powder obtained from *Pleoticus muelleri*'s shrimps. **(B–C).** Electronic microscopies images and their corresponding Fiji software analysis made on the magnifications. **B. SEM.** Black arrowhead: smooth edges, yellow arrowhead: agglomerates and small crystals. **C. TEM.** A complex fiber network that creates a slight roughness surface is observed between the peaks (yellow asterisks) and valleys intensities (black asterisks). For interpretation of the references to color in this figure legend, the reader is referred to the Web version of this article.

#### 2.5.3. Trypan Blue assay

Trypan Blue (TB) is an anionic hydrophilic azo dye that crosses the cell membranes of dead cells only, thereby staining dead tissues/cells blue [28]. For TB assay, the total number of viable and dead cells were counted using exclusion method as previously described [26]. Dead cells take up TB, meanwhile live cells exclude it. Then, the number of viable and dead cells was counted manually using a haemocytometer.

### 2.6. H-CS uptake

Eukaryotic cell lines were seeded on coverslips in plastic dishes. Upon reached the optimal confluence, cells were treated with H-CS couple with the Cyanine (Cyn) fluorescent probe (50 μg/mL), according to Ref. [16]. After 24 h, culture media was removed, and cells were washed with PBS and fixed with 4% paraformaldehyde. CLSM images were acquired in a FV1000 module CLSM (Olympus Inc., Japan) ($\lambda_{ex}$: 650 nm; $\lambda_{em}$: 780 nm). From the acquisition of CLSM images, 3D reconstruction was created using 3D Volume (Fiji software, NIH).

### 2.7. Statistical analysis

Experiments were carried out in triplicate unless otherwise stated. Results are expressed as Mean ± SEM. Comparisons between treatments were made by t-Student's test or 2-way ANOVA with interactions (concentration and diluent) in a completely randomized design. The assumptions of normality and homoscedasticity were studied analytically by the Shapiro-Wilks and the Levene tests, respectively. Tukey's test was used for *post hoc* comparisons. Results were considered significant at $p < 0.05$. GraphPad Prism 7 software (San Diego, USA) was used for data analyses.

## 3. Results

### 3.1. Characterization of H-CS

The macroscopic aspect of CS powder extracted from *Pleoticus muelleri*'s exoskeletons before and after the purified process is presented in Fig. 1A. H-CS ultrastructure was further examined by SEM and TEM analysis. The former revealed surface with smooth-edged agglomerates and small crystals (Fig. 1B). TEM images confirmed a detailed structure that comprises a complex fiber network that creates a slight roughness surface, which can be visualized as peaks and valleys intensities. The description presented above, was confirmed by surface isolines analysis and a digital 3D profile surface structure from SEM and TEM images respectively (Fig. 1C).

### 3.2. Biocompatibility studies of H-CS in prokaryotic cells

We tested whether H-CS had any effect on *L. casei* BL23 cellular proliferation or viability. None of the tested concentrations manifested one of the mentioned effects on the number of *L. casei*'s UFC/ml (Fig. 2A). At the same time, neither PBS (pH 7.4) nor $CH_3COOH$ 1% (w/v) solution influenced on the cell viability ($p > 0.05$).

CLSM images of living bacteria after staining with CFSE are shown in Fig. 2B. As expected, neither morphological nor density differences were observed when H-CS solutions with concentrations ranging from 0 to 50 μg/mL were added.

### 3.3. Biocompatibility studies of H-CS in eukaryotic cells

#### 3.3.1. Cytotoxicity testing

Cytotoxicity evaluation using cell culture-based methods provides a

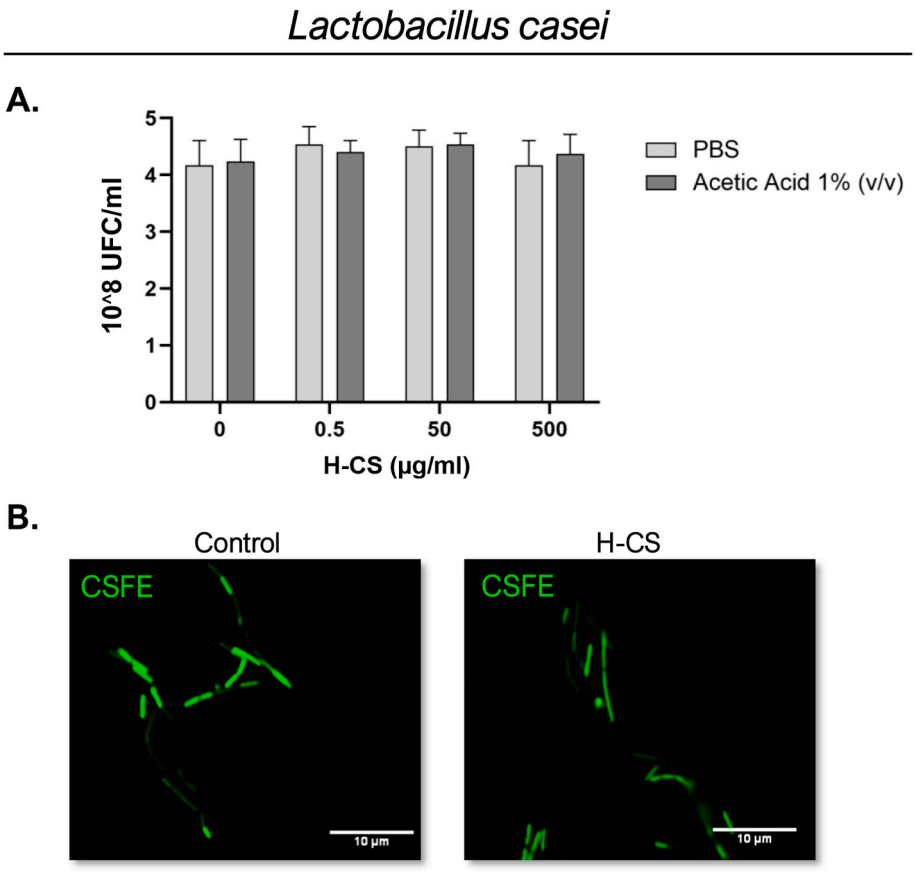


**Fig. 2. A.** Mean of *L. casei* Colony Forming Units per milliliter (CFU/mL) ± SEM. 2-Way ANOVA with interactions ($p > 0.05$). **B.** CLSM imaging of living *L. casei* incubated with 0 and 50 μg/mL of H-CS.

rough approach of the cell ability to survive in the presence of specific materials or vehicles. Depending on which cellular characteristics is centred, the method described to evaluate the biomaterial is mainly categorized into metabolic assays and membrane integrity assays [29,30]. Hence, a combination of different assays can provide a more comprehensive determination in the screening of material biocompatibility [3].

For 3T3-L1 mouse fibroblasts, we found a significant cell proliferation increase after H-CS treatment (Fig. 3). By means of both MTT and CV assays, the viability estimated was 21% and 26% higher for H-CS treated-cells than for the control cells, respectively (Fig. 3A, i and ii). On the other hand, TB exclusion analyses showed 31% and 50% increase in the number of total viable cells for 24 and 48 h, respectively, versus the control cells (Fig. 3A, iii). These results indicate that the supplementation of culture media with H-CS, at 10% FBS, was not only innocuous for fibroblast growth, but also increased cell proliferation. The mentioned effect on cell viability was also noted by observation of contrast microscopic images showing the cells growing at high densities upon H-CS addition (Fig. 3A, iv). Also, a considerable uptake of Cyn-H-CS molecules by 3T3-L1 cells was observed in CLSM images. In a complementary way, the 3D images reconstruction generated from the original ones allowed to confirm the presence of the dye fully colocalizing with cytoplasm, evidenced by the high levels of fluorescence (Fig. 3B).

Considering that native CS, as well as its derivatives polymers, has been frequently tested by means of MTT assay [30], we next continued with this methodology for human cell lines (Fig. 4). Through this metabolic assay and phase-contrast microscopy, a significant proliferation was determined in both Caco-2 (38%) and ARPE-19 (40%) cell lines, after H-CS treatment, (Fig. 4A, i and ii). On the contrary, MTT assay and microscopic images showed no significant differences in cell viability of EA.hy926 cells and in their density upon H-CS addition.

Based on these findings, we hypothesized that the obtained difference in proliferation could be linked to a differential cellular uptake. To corroborate it, we selected ARPE-19 in which proliferation was observed and EA. hy926 cells with the opposite behaviour. Notably, both cell lines fully incorporated Cyn-H-CS molecules (Fig. 4B), with a similar

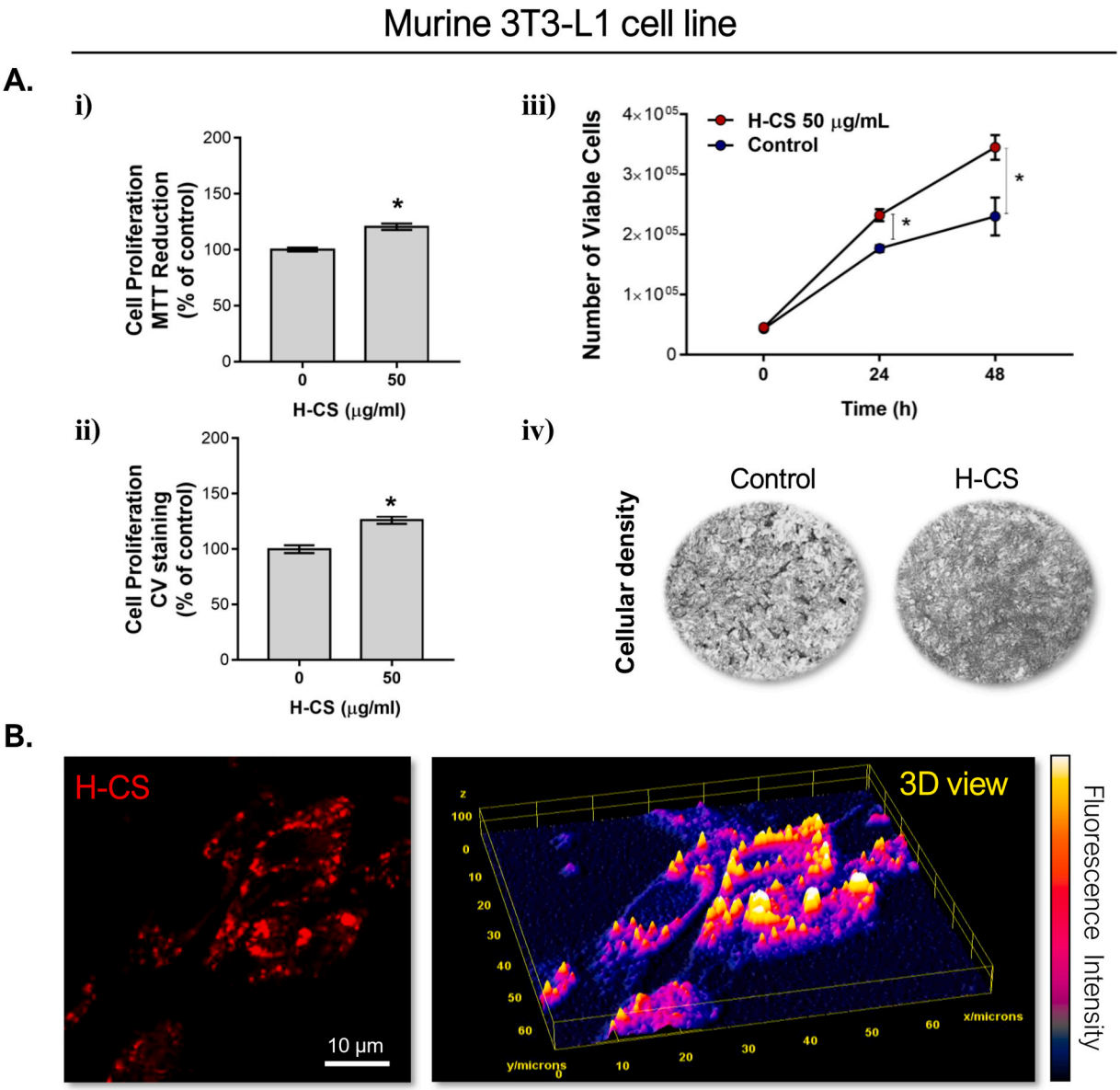


**Fig. 3. A.** Cell proliferation and viability assays for 3T3-L1 fibroblasts under H-CS treatment by means of MTT (i), Crystal violet (ii), TB exclusion (iii) and phase-contrast microscopy (iv) analysis. **B.** CLSM image showing Cyn-H-CS (50 μg/mL) uptake and the corresponding fluorescence intensity plot in 3D view. *$p < 0.01$ vs control. (For interpretation of the references to color in this figure legend, the reader is referred to the Web version of this article.)

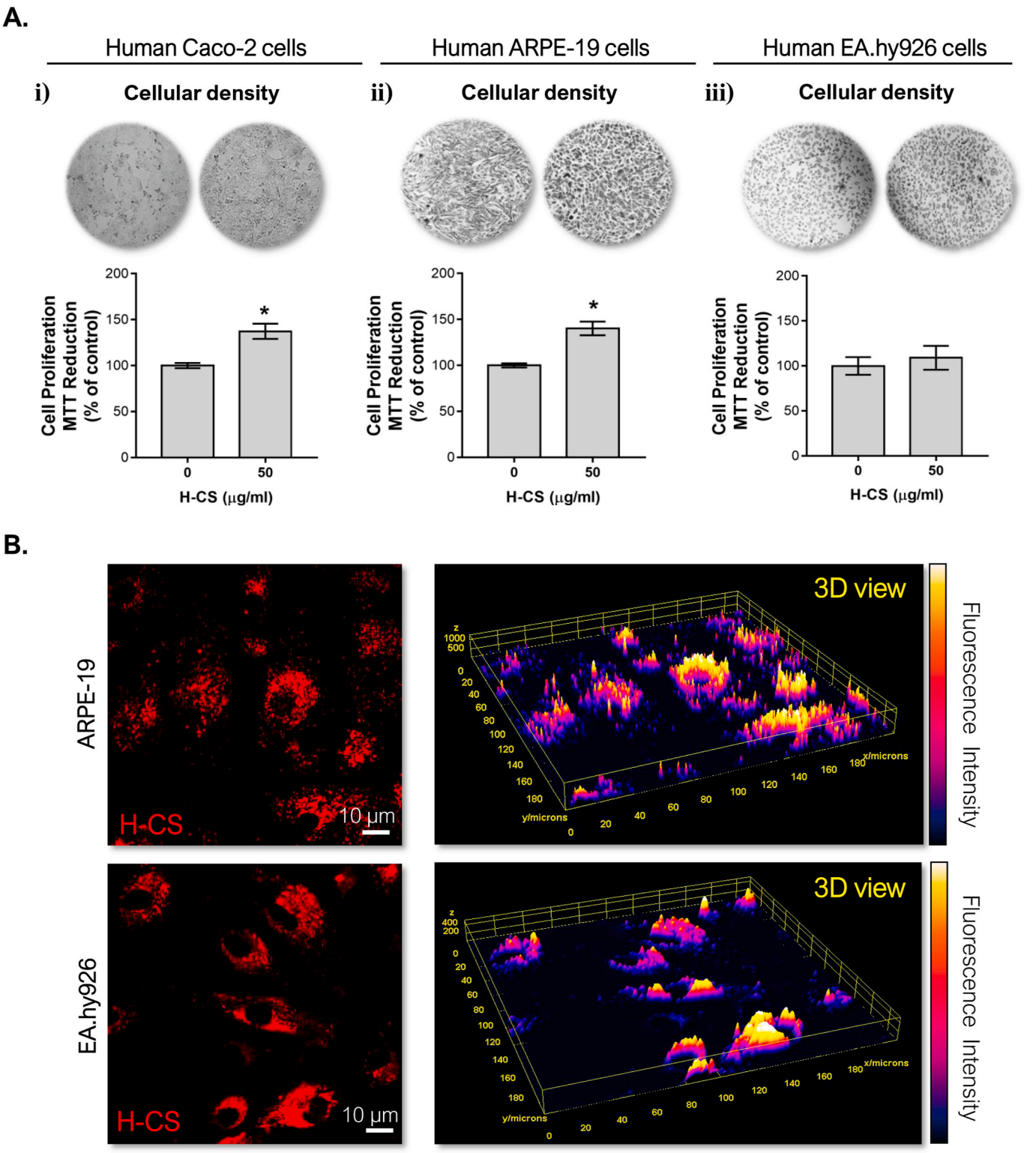


**Fig. 4. A.** MTT analysis and phase-contrast microscopy images corresponding to human Caco-2 (i), ARPE-19 (ii) and EA. hy926 (iii) cell lines. **B.** CLSM images showing Cyn-H-CS (50 μg/mL) uptake and the corresponding fluorescence intensity plots in 3D view. *$p < 0.01$ vs control.

behaviour to that described above for murine cells. Therefore, the proliferation effect cannot be explained just by the simple uptake into the cells. Thus, the present results constitute the bases for further mechanistic studies of the H-CS-induced proliferation to be addressed in a next contribution.

### 3.3.2. *Cell adhesion and morphology*

Another parameters to define the cytotoxicity of a biomaterial are both the cell adhesion and morphology, since they are probably the most valuable aspects of the cellular interaction with a biomaterial [4]. None of the mammalian lines studied exhibited changes in their morphology and adhesion. In a qualitative way, parameters observed and considered as healthy cultures are summed up in the following paragraphs (Fig. S1):

3T3-L1 cells showed fibroblast-like phenotype which includes thin and elongated (spindle-shaped) cells with a remarkably smooth cell surface. These cells grow characteristically in superimposed layers and typical cell morphologies indicative of cellular stress and/or toxicity include a decrease in cell size, cell detachment and reduction in confluence [31]; none of the mentioned events were detected upon H-CS treatment.

Caco-2 cells normally exhibit morphological differences with the increasing of passage number. Under our conditions, cells with 60–70 passages, normal cultures were observed which contained flatten and squamous cells whose contours were slightly defined, accordingly to Ref. [32]. As expected, Caco-2 culture progressed into flat islands, expanding over time, with granules corresponding to the glycogen storage [33]. When this culture is injured, cells start to shrink and round and lose their capacity to adhesion on the surface of the cultivation plate [34,35]. Under H-CS treatment, we observed no changes in the Caco-2 monolayer, without any disruption.

ARPE-19 cells showed flattened epithelial cobblestone-like morphology. Also, these cells attain reminiscent fibroblasts morphology after reaching confluence. Those characteristics were in accordance to previous descriptions [36,37]. Of note, when ARPE-19 cells were injured, rounded, shrunken and loosely attached cells with floating cells in the culture media used to appeared [27,38].

EA.hy926 cells remain growing as a population of large, closely opposed, polygonal cells with a centrally located nucleus and indistinct cell borders, which constitute a normal morphological phenotype [39]. Previous reports indicate that EA.hy926 cell changes, from a polygonal shape to a spindle-shape, are precedent to cell dead and detachment, upon cytotoxic treatments [40]. The mentioned characteristics were never observed for cells treated with H-CS.

## 4. Discussion

Biomaterials were employed from ancient times; however, in recent years, their degree of complexity has substantially grown making them to acquire a relevant position in many fields [41]. In the food industry, biomaterials could be exploited as edible films packaging, coating applications for probiotic bacteria, etc [42,43]. In the biomedical field, the biomaterial uses include the supporting, enhancing, or replacing damaged tissue or a biological function [5,44,45].

Among the wide spectrum of biomaterials, we centred on biopolymers, which are obtained from the living organisms (e.g. CS) [12,14]. Although polymer-based crosslinked materials are highly promising in the above-mentioned areas, the current proposals are focused mainly on commercial biomaterials. Since the employment of CS is not far behind the latest issue, it is essential to achieve a perfect balance between an environmental sustainability and functional use of this biomaterial [46]. In this sense, it is highly useful to recycle crustacean wastes originating from every corner of planet Earth and our research laboratory has joined to this sustainable motivation.

CS MW is an important attribute that greatly affects its physicochemical and biological properties, which ultimately will influence its application. Usually, there is a trend in scientific research to use low MW-CS. The MW of CS is proportional to its viscosity. The degree of deacetylation of chitosan is another relevant characteristic for this biopolymer [47,48]. The H-CS employed in this work present medium-deacetylation degree, like those commercials [20].

Nowadays, little information is found regarding to single CS in literature. The ultrastructure analysis of the employed H-CS revealed a slight roughness surface constituted by an anastomosing network of microfibers (Fig. 1). Similar description was given for a CS derived from crayfish *Procambarus clarkii*'s exoskeleton wastes [48].

While drug molecules should be discussed in terms of toxicity, the biomedical materials, which include polymers, should be considered for their biocompatibility. More precisely, the biocompatibility of a material refers to its performance with a suitable host response in a particular situation [30].

In an elucidative review, Calinoiu *et al*. suggest that the most significant applications of CS in food industry comprise the coating material for probiotic stability with the aim of generate functional products, biodegradable films, food conservation from microbial deterioration or bacteriophages, etc [43]. Probiotics are live microorganisms widely used as nutraceutical products for the supplementation of intestinal flora [49,50]. The well-balanced gut microbiota is crucial in preserving human health and ought to not be modified by the intake of probiotics coated with biomaterials [50]. Among the widely probiotics present in the intestinal flora, the genus *Lactobacillus* is biotechnologically more suitable for food applications. Remarkably, diverse species of *Lactobacillus* have emerged as vectors for the release of antigens through the gastro-intestinal epithelium. In particular, *L. casei* is present in the human intestinal flora and is a widely studied species [25]. Present results showed that H-CS did not evoke appreciable adverse effects on the growth of lactic acid bacteria colonies. Similarly, another lactic acid producing probiotics like *L. plantarum*, *L. acidophilus*, *L. bulgaricus* [50] and *Bacillus coagulans* [51] were protected by CS and alginate. Hence, our results suggest that H-CS offers a promising matrix to deliver probiotics since it would reduce the problems generated by bacteriophages in the dairy industry as well as allow to increase the residence time of bacteria in the gastrointestinal mucosa, given the mucoadhesive properties of CS. In this sense, our work also explored the effect of H-CS on human intestinal cells (Caco-2), being able to verify its biocompatibility.

In Caco-2 cells, the cytotoxic and potentially anti-proliferative effect of CS-derived formulations; e.g. CS-nanoparticles [52,53], CS-nanocomposites [54] and chemically modified-CS [55], were previously evaluated in order to assess their biocompatibility and their subsequent potential use as drug delivery carriers for oral administrations. Low viscosity CS was evaluated on its free form, showing no harmful effects in Caco-2 cells and even an increased cell proliferation, similarly to this work [56]. The cellular and molecular pathways that regulate this CS-induced proliferation in Caco-2 cells remain unknown. Loh *et al.* [52] reported an effect of pH condition of CS treatments; medium size-CS at pH 6.0 applied for 72 h increased Caco-2 proliferation in comparison to pH 7.4 condition. In contrast, CS that has been chemically modified to increase their solubility in water (quaternized CS), shows some negative effects on proliferation by decreasing cell viability [55].

CS has been broadly proposed for biomedical and pharmaceutical uses, such as drug/gene/vaccine delivery, tissue engineering, wound healing, and cosmetic products. In this sense, CS could solve the disadvantages and obstacles in the process of drug transportation [17,57]. Such is the case of various routes of administration, which involve different types of cells and with which the biomaterial must interact. Data from the present report allow us to suggest that H-CS would be a promissory vehicle for ocular and dermal drug delivery. We determined that retinal pigment epithelium, as well as fibroblast and endothelial cells, exhibited a suitable cellular response reflected by biocompatibility and effective uptake of the H-CS.

Adhesion and proliferation of human dermal fibroblasts were stimulated by Icelandic marine CS [58] and Korean CS [59]. The latter work hypothesized that the free amine would play a crucial role in both cellular events. Also, it should be note, that the rough-prone surface of CS was previously related with cell adhesion and proliferation tendency [60]. Silva *et al.* proposed that CS could have an intrinsic mitogenic activity, similar to a competent growth factor [61]. The survey of previous studies indicates that the intrinsic mitogenic activity of CS is controversial and depends on the nature of the biopolymer and the specific testing conditions and cell lines used [61,62]. On the contrary, an inhibitory effect on mitogenesis was previously reported for CS molecules in skin fibroblasts [63]. Cell adhesion increases were reported as a CS effect improving cell behaviour in 2D culture systems [64].

Endothelial cells, in the blood vessels, exert regulatory functions whereby comprise therapeutic targets employed for the treatment of many pathologies [65]. A prominent feature of cardiovascular disease is

an enhanced oxidative damage and CS resulted in protection of endothelial cells from human umbilical vein after hydrogen peroxide-induced apoptosis [66]. Experiments with CS-based liposomal thermogels, designed for an effective drug delivery in the treatment of vascular malformation disease, resulted in normal viability rate and cell morphology for EA.hy926 cell line [67]. Previous results indicated that while CS alone favoured cell attachment and growth of human coronary artery endothelial cells, glycosaminoglycans-CS materials inhibited cell spreading and proliferation; meanwhile, dextran sulfate-CS stimulated cell proliferation [7]. On the other hand, murine bEnd5 brain endothelial cells showed no proliferation under commercial CS treatment [68]. As evidenced, there are many disparities about the cell growth behaviour depending on the type of CS used and the cell lines cultured. Together, these findings denote how relevant could be the selection of *in vitro* experimental models. As indicated by Martín-López *et al.*, cell growth depend not only on the molecular characteristics of CS but also on intrinsic factors of the employed cell type under study [68].

For ARPE-19 cells, the biocompatibility of non-cross-linked CS membranes from crab shells was demonstrated by the absence of any signs of cytotoxicity, although no changes in cell proliferation were reported [69]. Noorani *et al.* obtained that gelatin-CS induced an optimal cellular attachment and proliferation and suggest a compatible interaction of the biomaterial with human retinal pigment epithelium (RPE) cells [70]. On the other hand, ARPE-19 cells cell viability did not change it growth rate after the addition of CS oligosaccharides (5000 Da) to culture media [71].

It is relevant to highlight that the eye is conformed with quite a few regulatory mechanisms to avoid inflammatory and immune responses. For this reason, this organ is considered as an immune privileged microenvironment. Particularly, the RPE plays a pivotal role in retinal immunity since it constitutes part of the blood-eye barrier. Under inflammatory conditions, RPE cells produce a myriad of cytokines that may activate the resident ocular cells or attract and activate resident macrophages/microglial cells. In addition, immunoregulatory functions of RPE cells are achieved, toll-like receptor activation, nitric oxide secretion, complement regulation and antigen presentation. In sum, the RPE cell coordinates both innate and adaptive immunity and comprises a plethora of factors to regulate the immune response [72–75]. Considering the relevant role of RPE cells in the immunogenic response, we recently determined the levels of pro-inflammatory interleukin cytokines after H-CS treatment. Our findings revealed that H-CS did not stimulated the secretion of IL-6 and IL-8 in ARPE-19 [76].

In summary, the present work contributes to the understanding of H-CS interactions with biological elements, such as bacteria and eukaryotic cells. This knowledge may be exploited for biomedical, cosmetic, nutraceutical or food industry applications.

## Author contributions

O.E.P directed the study. M.C.DS, A.A, A.P.D.R, and O.E.P. contributed to the design and interpretation of the experimental results, wrote, and edited the manuscript. M.C.DS, A.P.DR, R. DM and A.A executed experiments. All authors read and approved the final manuscript.

## Author statement

- Oscar Edgardo Pérez directed the study.
- Mariana Carolina Di Santo, Agustina Alaimo, Ana Paula Domínguez Rubio and Oscar Edgardo Pérez contributed to the design and interpretation of the experimental results, wrote, and edited the manuscript.
- Mariana Carolina Di Santo, Agustina Alaimo, Ana Paula Domínguez Rubio and Regina De Matteo executed experiments.

## Declaration of competing interest

The authors declare that there is no conflict of interest.

## Acknowledgments

A.A, A.P.DR and O.E.P are members of the Research Career from CONICET. M.C.DS and R.DM are fellows from ANPCyP and CONICET, respectively.

## Appendix A. Supplementary data

Supplementary data to this article can be found online at https://doi.org/10.1016/j.bbrep.2020.100842.

## References

[1] O.O. Ige, L.E. Umoru, S. Aribo, Natural products: a minefield of biomaterials, ISRN Mater. Sci. (2012) 1–20, https://doi.org/10.5402/2012/983062.
[2] B.D. Ulery, L.S. Nair, C.T. Laurencin, Biomedical applications of biodegradable polymers, J. Polym. Sci., Part B: Polym. Phys. 49 (2011) 832–864, https://doi.org/10.1002/polb.22259.
[3] M. Bernard, E. Jubeli, M.D. Pungente, N. Yagoubi, Biocompatibility of polymer-based biomaterials and medical devices-regulations,: in vitro screening and risk-management, Biomater. Sci. 6 (2018) 2025–2053, https://doi.org/10.1039/c8bm00518d.
[4] C.J. Kirkpatrick, F. Bittinger, M. Wagner, H. Kohler, T.G. Van Kooten, C.L. Klein, M. Otto, Current trends in biocompatibility testing, Proc. Inst. Mech. Eng. Part H J. Eng. Med. 212 (1998) 75–84, https://doi.org/10.1243/0954411981533845.
[5] H.F. Oldenkamp, J.E.V. Ramirez, N.A. Peppas, Re-evaluating the importance of carbohydrates as regenerative biomaterials, Regen. Biomater. 6 (2019) 1, https://doi.org/10.1093/RB/RBY023.
[6] F.G. Torres, O.P. Troncoso, A. Pisani, F. Gatto, G. Bardi, Natural polysaccharide nanomaterials: an overview of their immunological properties, Int. J. Mol. Sci. 20 (2019), https://doi.org/10.3390/ijms20205092.
[7] J.M. Chupa, A.M. Foster, S.R. Sumner, S.V. Madihally, H.W. Matthew, Vascular cell responses to polysaccharide materials, Biomaterials 21 (2000) 2315–2322, https://doi.org/10.1016/s0142-9612(00)00158-7.
[8] P. Manivasagan, J. Oh, Marine polysaccharide-based nanomaterials as a novel source of nanobiotechnological applications, Int. J. Biol. Macromol. 82 (2016) 315–327, https://doi.org/10.1016/j.ijbiomac.2015.10.081.
[9] M.K. Sarangi, M.E.B. Rao, V. Parcha, D.K. Yi, S.S. Nanda, Marine polysaccharides for drug delivery in tissue engineering, Nat. Polysaccharides Drug Deliv. Biomed. Appl. (2019) 513–530, https://doi.org/10.1016/B978-0-12-817055-7.00022-4. Elsevier.
[10] Y.E. Lee, H. Kim, C. Seo, T. Park, K. Bin Lee, S.Y. Yoo, S.C. Hong, J.T. Kim, J. Lee, Marine polysaccharides: therapeutic efficacy and biomedical applications, Arch Pharm. Res. (Seoul) 40 (2017) 1006–1020, https://doi.org/10.1007/s12272-017-0958-2.
[11] N.H.K. Al Shaqsi, H.A.S. Al Hoqani, M.A. Hossain, M.A. Al Sibani, Optimization of the demineralization process for the extraction of chitin from Omani Portunidae segnis, Biochem. Biophys. Reports. 23 (2020), 100779, https://doi.org/10.1016/j.bbrep.2020.100779.
[12] D. Elieh-Ali-Komi, M.R. Hamblin, Chitin and chitosan: production and application of versatile biomedical nanomaterials, Int. J. Adv. Res. 4 (2016) 411–427.
[13] C. Schmitz, L.G. Auza, D. Koberidze, S. Rasche, R. Fischer, L. Bortesi, Conversion of chitin to defined chitosan oligomers: current status and future prospects, Mar. Drugs 17 (2019), https://doi.org/10.3390/md17080452.
[14] G. Crini, Historical review on chitin and chitosan biopolymers, Environ. Chem. Lett. 17 (2019) 1623–1643, https://doi.org/10.1007/s10311-019-00901-0.
[15] Z. Shariatinia, Pharmaceutical applications of chitosan, Adv. Colloid Interface Sci. 263 (2019) 131–194, https://doi.org/10.1016/j.cis.2018.11.008.
[16] M.C. Di Santo, A. Alaimo, L.S. Acebedo, C. Spagnuolo, R. Pozner, O.E. Pérez, Biological responses induced by high molecular weight chitosan administrated jointly with Platelet-derived Growth Factors in different mammalian cell lines, Int. J. Biol. Macromol. 158 (2020) 953–967, https://doi.org/10.1016/j.ijbiomac.2020.05.032.
[17] S.K. Shukla, A.K. Mishra, O.A. Arotiba, B.B. Mamba, Chitosan-based nanomaterials: a state-of-the-art review, Int. J. Biol. Macromol. 59 (2013) 46–58, https://doi.org/10.1016/j.ijbiomac.2013.04.043.
[18] T. Groth, P. Falck, R.R. Miethke, Cytotoxicity of biomaterials - basic mechanisms and in vitro test methods: a review, ATLA Altern. to Lab. Anim. 23 (1995) 790–799, https://doi.org/10.1177/026119299502300609.
[19] L.C. Keong, A.S. Halim, In Vitro models in biocompatibility assessment for biomedical-grade chitosan derivatives in wound management, Int. J. Mol. Sci. 10 (2009) 1300–1313, https://doi.org/10.3390/ijms10031300.
[20] C.R. Prudkin Silva, J.H. Martínez, K.D. Martínez, M.E. Farías Hermosilla, F. Coluccio Leskow, O.E. Pérez, Proposed molecular model for electrostatic interactions between insulin and chitosan . Nano-complexation and activity in cultured cells Proposed molecular model for electrostatic interactions between

insulin and chitosan . Nano-complexation and activity i, Colloids Surf., A 537 (2017) 425–434, https://doi.org/10.1016/j.colsurfa.2017.10.040.
[21] C. Prudkin-Silva, O.E. Pérez, K.D. Martínez, F.L. Barroso da Silva, Combined experimental and molecular simulation study of insulin–chitosan complexation driven by electrostatic interactions, J. Chem. Inf. Model. (2020), https://doi.org/10.1021/acs.jcim.9b00814.
[22] J. Li, Y. Wu, L. Zhao, Antibacterial activity and mechanism of chitosan with ultra high molecular weight, Carbohydr. Polym. 148 (2016) 200–205, https://doi.org/10.1016/j.carbpol.2016.04.025.
[23] S. Sreekumar, F.M. Goycoolea, B.M. Moerschbacher, G.R. Rivera-Rodriguez, Parameters influencing the size of chitosan-TPP nano- and microparticles, Sci. Rep. 8 (2018) 1–11, https://doi.org/10.1038/s41598-018-23064-4.
[24] A.M. Safer, S. Leporatti, J. Jose, M.S. Soliman, Conjugation of EGCG and chitosan NPS as a novel nano-drug delivery system, Int. J. Nanomed. 14 (2019) 8033–8046, https://doi.org/10.2147/IJN.S217898.
[25] A.P. Domínguez Rubio, J.H. Martínez, D.C. Martínez Casillas, F. Coluccio Leskow, M. Piuri, O.E. Pérez, Lactobacillus casei BL23 produces microvesicles carrying proteins that have been associated with its probiotic effect, Front. Microbiol. 8 (2017) 1783, https://doi.org/10.3389/fmicb.2017.01783.
[26] K.S.K.S. Louis, A.C.A.C. Siegel, Mammalian cell viability, Methods Mol. Biol. 740 (2011) 7–12, https://doi.org/10.1007/978-1-61779-108-6.
[27] A. Alaimo, M.C. Di Santo, A. Domínguez Rubio, G. Chaufan, G. García Liñares, O. E. Pérez, Toxic effects of A2E in human ARPE - 19 cells were prevented by resveratrol : a potential nutritional bioactive for age - related macular degeneration treatment, Arch. Toxicol. 94 (2020) 553–562, https://doi.org/10.1007/s00204-019-02637-w.
[28] M.E. Farah, M. Maia, F.M. Penha, E.B. Rodrigues, The use of vital dyes during vitreoretinal surgery – chromovitrectomy, Retin. Pharmacother. (2010) 331–335, https://doi.org/10.1016/b978-1-4377-0603-1.00053-3. Elsevier.
[29] Ö.S. Aslantürk, In vitro cytotoxicity and cell viability assays: principles, advantages, and disadvantages, in: Genotoxicity - A Predict. Risk to Our Actual World, InTech, 2018, https://doi.org/10.5772/intechopen.71923.
[30] S. Rodrigues, M. Dionísio, C.R. López, A. Grenha, Biocompatibility of chitosan carriers with application in drug delivery, J. Funct. Biomater. 3 (2012) 615–641, https://doi.org/10.3390/jfb3030615.
[31] T. Vertigan, K. Dunlap, A. Reynolds, L. Duffy, Effects of methylmercury exposure in 3T3-L1, Adipocytes 4 (2017) 94–111, https://doi.org/10.3934/environsci.2017.1.94.
[32] K.A. Jahn, J.M. Biazik, F. Braet, GM1 expression in caco-2 cells: characterisation of a fundamental passage-dependent transformation of a cell line, J. Pharmacol. Sci. 100 (2011) 3751–3762, https://doi.org/10.1002/jps.22418.
[33] A. Ferraretto, C. Gravaghi, E. Donetti, S. Cosentino, B.M. Donida, M. Bedoni, G. Lombardi, A. Fiorilli, G. Tettamanti, New methodological approach to induce a differentiation phenotype in Caco-2 cells prior to post-confluence stage, Anticancer Res. 27 (2007) 3919–3925.
[34] E.A. Elsayed, M.A. Sharaf-Eldin, M. Wadaan, In vitro evaluation of cytotoxic activities of essential oil from Moringa oleifera seeds on HeLa, HepG2, MCF-7, CACO-2 and L929 cell lines, Asian Pac. J. Cancer Prev. APJCP 16 (2015) 4671–4675, https://doi.org/10.7314/APJCP.2015.16.11.4671.
[35] G. Chakrabarti, X. Zhou, B.A. McClane, Death pathways activated in CaCo-2 cells by Clostridium perfringens enterotoxin, Infect. Immun. 71 (2003) 4260–4270, https://doi.org/10.1128/IAI.71.8.4260-4270.2003.
[36] K.C. Dunn, A.E. Aotaki-Keen, F.R. Putkey, L.M. Hjelmeland, ARPE-19 , A human retinal pigment epithelial cell line with, Exp. Eye Res. (1996), https://doi.org/10.1006/exer.1996.0020.
[37] W. Samuel, C. Jaworski, O.A. Postnikova, R.K. Kutty, T. Duncan, L.X. Tan, E. Poliakov, A. Lakkaraju, T.M. Redmond, Appropriately differentiated ARPE-19 cells regain phenotype and gene expression profiles similar to those of native RPE cells, Mol. Vis. 23 (2017) 60–89.
[38] J. Li, J. Sun, B. Li, Z. Liu, Astaxanthin protects ARPE-19 cells against oxidative stress injury induced by hydrogen peroxide, Biotechnol. Biotechnol. Equip. 32 (2018) 1277–1284, https://doi.org/10.1080/13102818.2018.1512378.
[39] E.A. Jaffe, R.L. Nachman, C.G. Becker, C.R. Miinick, Culture of Human Endothelial Cells Derived from Umbilical Veins 52 (1973) 2745–2756.
[40] L. Nelimarkka, V. Kainulainen, E. Scho, S. Moisander, M. Jortikka, M. Lammi, K. Elenius, M. Jalkanen, H. Ja, Expression of small extracellular chondroitin/dermatan sulfate proteoglycans is differentially regulated in human endothelial cells * 272 (1997) 12730–12737.
[41] N. Huebsch, D.J. Mooney, Inspiration and application in the evolution of biomaterials, Nature 462 (2009) 426–432, https://doi.org/10.1038/nature08601.
[42] R. Grujic, M. Vukic, V. Gojkovic, Application of biopolymers in the food industry, in: Adv. Appl. Ind. Biomater, Springer International Publishing, 2017, pp. 103–119, https://doi.org/10.1007/978-3-319-62767-0_6.
[43] L.F. Calinoiu, B.E. Ştefanescu, I.D. Pop, L. Muntean, D.C. Vodnar, Chitosan coating applications in probiotic microencapsulation, Coatings 9 (2019) 1–21, https://doi.org/10.3390/COATINGS9030194.
[44] D. Zhao, S. Yu, B. Sun, S. Gao, S. Guo, K. Zhao, Biomedical applications of chitosan and its derivative nanoparticles, Polymers 10 (2018), https://doi.org/10.3390/polym10040462.
[45] L. Gu, T. Shan, Y. xuan Ma, F.R. Tay, L. Niu, Novel biomedical applications of crosslinked collagen, Trends Biotechnol. 37 (2019) 464–491, https://doi.org/10.1016/j.tibtech.2018.10.007.
[46] H.E. Ghannam, A.S. Talab, N.V. Dolgano, A.M.S. Husse, N.M. Abdelmagui, Characterization of chitosan extracted from different Crustacean shell wastes, J. Appl. Sci. 16 (2016) 454–461, https://doi.org/10.3923/jas.2016.454.461.
[47] X. He, K. Li, R. Xing, S. Liu, L. Hu, P. Li, The production of fully deacetylated chitosan by compression method, Egypt, J. Aquat. Res. 42 (2016) 75–81, https://doi.org/10.1016/j.ejar.2015.09.003.
[48] M.M. El-Naggar, W.S.I. Abou-Elmagd, A. Suloma, H.A. El-Shabaka, M.T. Khalil, F. A. Abd El-Rahman, Optimization and physicochemical characterization of chitosan and chitosan nanoparticles extracted from the crayfish Procambarus clarkii wastes, J. Shellfish Res. 38 (2019) 385, https://doi.org/10.2983/035.038.0220.
[49] A.P. Dominguez Rubio, J. Martínez, M. Palavecino, F. Fuentes, C.M.S. López, A. Marcilla, O.E. Pérez, M. Piuri, Transcytosis of Bacillus subtilis extracellular vesicles through an in vitro intestinal epithelial cell model, Sci. Rep. 10 (2020) 1–12, https://doi.org/10.1038/s41598-020-60077-4.
[50] M.A. Khalil, M.M. El-Sheekh, H.I. El-Adawi, N.M. El-Deeb, M.Z. Hussein, Efficacy of microencapsulated lactic acid bacteria in helicobater pylori eradication therapy, J. Res. Med. Sci. 20 (2015) 950–957, https://doi.org/10.4103/1735-1995.172782.
[51] A.C. Anselmo, K.J. McHugh, J. Webster, R. Langer, A. Jaklenec, Layer-by-Layer encapsulation of probiotics for delivery to the microbiome, Adv. Mater. 28 (2016) 9486–9490, https://doi.org/10.1002/adma.201603270.
[52] J.W. Loh, M. Saunders, L.Y. Lim, Cytotoxicity of monodispersed chitosan nanoparticles against the Caco-2 cells, Toxicol. Appl. Pharmacol. 262 (2012) 273–282, https://doi.org/10.1016/j.taap.2012.04.037.
[53] H.J. Je, E.S. Kim, J.S. Lee, H.G. Lee, Release properties and cellular uptake in caco-2 cells of size-controlled chitosan nanoparticles, J. Agric. Food Chem. 65 (2017) 10899–10906, https://doi.org/10.1021/acs.jafc.7b03627.
[54] J. Kowapradit, P. Opanasopit, T. Ngawhirunpat, A. Apirakaramwong, T. Rojanarata, U. Ruktanonchai, W. Sajomsang, In Vitro Permeability Enhancement in Intestinal Epithelial Cells (Caco-2) Monolayer of Water Soluble Quaternary Ammonium Chitosan Derivatives, vol. 11, 2010, https://doi.org/10.1208/s12249-010-9399-7.
[55] R. Wongwanakul, S. Jianmongkol, Biocompatibility Study of Quaternized Chitosan on the Proliferation and Differentiation of Caco-2 Cells as an in Vitro Model of the Intestinal Barrier, 2016, https://doi.org/10.1177/0883911516658780.
[56] I. Salcedo, C. Aguzzi, G. Sandri, M.C. Bonferoni, M. Mori, P. Cerezo, R. Sánchez, C. Viseras, C. Caramella, In vitro biocompatibility and mucoadhesion of montmorillonite chitosan nanocomposite : a new drug delivery, Appl. Clay Sci. 55 (2012) 131–137, https://doi.org/10.1016/j.clay.2011.11.006.
[57] J. Li, C. Cai, J. Li, J. Li, J. Li, T. Sun, L. Wang, H. Wu, G. Yu, Chitosan-based nanomaterials for drug delivery, Molecules 23 (2018), https://doi.org/10.3390/molecules23102661.
[58] V. Patrulea, N. Hirt-Burri, A. Jeannerat, L.A. Applegate, V. Ostafe, O. Jordan, G. Borchard, Peptide-decorated chitosan derivatives enhance fibroblast adhesion and proliferation in wound healing, Carbohydr. Polym. 142 (2016) 114–123, https://doi.org/10.1016/j.carbpol.2016.01.045.
[59] H.K. Chun, H.S. Park, J.G. Yong, Y. Son, S.H. Lim, J.C. Young, K.S. Park, W. P. Chan, Improvement of the biocompatibility of chitosan dermal scaffold by rigorous dry heat treatment, Macromol. Res. 12 (2004) 367–373, https://doi.org/10.1007/bf03218413.
[60] L.J.R. Foster, S. Ho, J. Hook, M. Basuki, H. Marçal, Chitosan as a biomaterial: influence of degree of deacetylation on its physiochemical, material and biological properties, PloS One 10 (2015), e0135153, https://doi.org/10.1371/journal.pone.0135153.
[61] D. Silva, R. Arancibia, C. Tapia, A. Na-Rougier, Diaz, chitosan and platelet-derived growth factor synergistically stimulate cell proliferation in gingival fibroblasts. https://doi.org/10.1111/jre.12053, 2013.
[62] H. Inui, M. Tsujikubo, S. Hirano, Low molecular weight chitosan stimulation of mitogenic response to platelet-derived growth factor in vascular smooth muscle cells, biosci, Biotechnol. Biochem. 59 (2009) 2111–2114, https://doi.org/10.1271/bbb.59.2111.
[63] G.I. Howling, P.W. Dettmar, P.A. Goddard, F.C. Hampson, M. Dornish, E.J. Wood, The effect of chitin and chitosan on the proliferation of human skin fibroblasts and keratinocytes in vitro, Biomaterials 22 (2001) 2959–2966, https://doi.org/10.1016/S0142-9612(01)00042-4.
[64] G.A.S. Kazi, T. Yamanaka, Y. Osamu, Chitosan coating an efficient approach to improve the substrate surface for in vitro culture system, J. Electrochem. Soc. 166 (2019) B3025–B3030, https://doi.org/10.1149/2.0051909jes.
[65] R.Y. Kiseleva, P.M. Glassman, C.F. Greineder, E.D. Hood, V.V. Shuvaev, V. R. Muzykantov, Targeting therapeutics to endothelium: are we there yet? Drug Deliv. Transl. Res. 8 (2018) 883–902, https://doi.org/10.1007/s13346-017-0464-6.
[66] H.T. Liu, J.L. He, W.M. Li, Z. Yang, Y.X. Wang, X.F. Bai, C. Yu, Y.G. Du, Chitosan oligosaccharides protect human umbilical vein endothelial cells from hydrogen peroxide-induced apoptosis, Carbohydr. Polym. 80 (2010) 1062–1071, https://doi.org/10.1016/j.carbpol.2010.01.025.
[67] L. Zhang, F. Chen, J. Zheng, H. Wang, X. Qin, W. Pan, Chitosan-based liposomal thermogels for the controlled delivery of pingyangmycin: design, optimization and in vitro and in vivo studies, Drug Deliv. 25 (2018) 690–702, https://doi.org/10.1080/10717544.2018.1444684.
[68] E. Martín-López, M. Nieto-Díaz, M. Nieto-Sampedro, Influence of Chitosan concentration on cell viability and proliferation in vitro by changing film topography, J. Appl. Biomater. Funct. Mater. 11 (2013) 151–158, https://doi.org/10.5301/JABFM.2012.10449.
[69] J. Lai, Y. Li, T. Wang, In Vitro Response of Retinal Pigment Epithelial Cells Exposed to Chitosan Materials Prepared with Different Cross-Linkers, 2010, pp. 5256–5272, https://doi.org/10.3390/ijms11125256.
[70] B. Noorani, F. Tabandeh, F. Yazdian, Z.S. Soheili, M. Shakibaie, S. Rahmani, Thin natural gelatin/chitosan nanofibrous scaffolds for retinal pigment epithelium cells,

Int. J. Polym. Mater. Polym. Biomater. 67 (2018) 754–763, https://doi.org/10.1080/00914037.2017.1362639.

[71] C.-W. Lin, H.-H. Huang, C.-M. Yang, C.-H. Yang, Protective effect of chitosan oligosaccharides on blue light light-emitting diode induced retinal pigment epithelial cell damage, J. Funct. Foods. 49 (2018) 12–19, https://doi.org/10.1016/j.jff.2018.08.007.

[72] G.M. Holtkamp, A. Kijlstra, R. Peek, A.F. De Vos, Retinal pigment epithelium-immune system interactions: cytokine production and cytokine-induced changes, Prog. Retin. Eye Res. 20 (2001) 29–48, https://doi.org/10.1016/S1350-9462(00)00017-3.

[73] B. Detrick, J.J. Hooks, The RPE cell and the immune system, in: Retin. Pigment Ep. Heal. Dis, Springer International Publishing, 2020, pp. 101–114, https://doi.org/10.1007/978-3-030-28384-1_6.

[74] H. Keino, S. Horie, S. Sugita, Immune privilege and eye-derived T-regulatory cells, J. Immunol. Res. 2018 (2018), https://doi.org/10.1155/2018/1679197.

[75] G.M. Holtkamp, M. Van Rossem, A.F. De Vos, B. Willekens, R. Peek, A. Kijlstra, Polarized Secretion of IL-6 and IL-8 by Human Retinal Pigment Epithelial Cells, 1998, https://doi.org/10.1046/j.1365-2249.1998.00560.x.

[76] F.S. Buosi, A. Alaimo, M.C. Di Santo, F. Elías, G. García Liñares, S.L. Acebedo, M. A. Castañeda Catañ, C.C. Spagnuolo, L. Lizarraga, K.D. Martínez, O.E. Pérez, Resveratrol encapsulation in high molecular weight chitosan-based nanogels for applications in ocular treatments: impact on human ARPE-19 culture cells, Int. J. Biol. Macromol. 165 (2020) 804–821, https://doi.org/10.1016/j.ijbiomac.2020.09.234.